Biochemical Pharmacology 80 (2010) 1033–1041

Contents lists available at ScienceDirect

Biochemical Pharmacology

journal homepage: www.elsevier.com/locate/biochempharm

Potency variation of small-molecule chymase inhibitors across species☆

Jukka Kervinen [1,*], Carl Crysler [1], Shariff Bayoumy, Marta C. Abad, John Spurlino, Ingrid Deckman, Michael N. Greco, Bruce E. Maryanoff, Lawrence de Garavilla [**]

Johnson & Johnson Pharmaceutical Research and Development, Welsh and McKean Roads, Spring House, PA 19477, United States

ARTICLE INFO

Article history:
Received 14 April 2010
Accepted 10 June 2010

Keywords:
Chymase
Inflammatory disease
Inhibitor potency
Mast cell protease (MCP)
X-ray structure

ABSTRACT

Chymases (EC 3.4.21.39) are mast cell serine proteinases that are variably expressed in different species and, in most cases, display either chymotryptic or elastolytic substrate specificity. Given that chymase inhibitors have emerged as potential therapeutic agents for treating various inflammatory, allergic, and cardiovascular disorders, it is important to understand interspecies differences of the enzymes as well as the behavior of inhibitors with them. We have expressed chymases from humans, macaques, dogs, sheep (MCP2 and MCP3), guinea pigs, and hamsters (HAM1 and HAM2) in baculovirus-infected insect cells. The enzymes were purified and characterized with kinetic constants by using chromogenic substrates. We evaluated *in vitro* the potency of five nonpeptide inhibitors, originally targeted against human chymase. The inhibitors exhibited remarkable cross-species variation of sensitivity, with the greatest potency observed against human and macaque chymases, with K_i values ranging from ~0.4 to 72 nM. Compounds were 10–300-fold less potent, and in some instances ineffective, against chymases from the other species. The X-ray structure of one of the potent phosphinate inhibitors, JNJ-18054478, complexed with human chymase was solved at 1.8 Å resolution to further understand the binding mode. Subtle variations in the residues in the active site that are already known to influence chymase substrate specificity can also strongly affect the compound potency. The results are discussed in the context of selecting a suitable animal model to study compounds ultimately targeted for human chymase.

1. Introduction

Activated mast cells secrete diverse pro-inflammatory mediators, including histamine, arachidonate metabolites, and proteases [1]. One of the proteases released is chymase (EC 3.4.21.39), a serine protease of the S1A family that promotes inflammation, matrix destruction, and tissue remodeling [2,3]. Human chymase has been linked to several pathophysiological events in mast cell-dependent inflammatory diseases, including asthma [4], Crohn's disease [5], atopic dermatitis [6] and vascular degeneration [7,8]. Cleavage of several endogenous substrates has been linked to the pathologic conditions. For example, degradation of high-density lipoprotein (HDL) by mast cell chymase and tryptase and activation of pro-MMP1 (interstitial collagenase) by chymase promote development of atherosclerotic lesions [7]. Whereas chymase is normally regulated by endogenous serine protease inhibitors (SERPINS), such as α1-antichymotrypsin and α1-proteinase inhibitor [9], inflamed tissues have decreased levels of these inhibitors. Moreover, chymase has been shown to cleave the endogenous secretory leukocyte protease inhibitor (SLPI) [10,11], which further contributes to the protease/protease inhibitor imbalance. Thus, agents that inhibit chymase could be useful as anti-inflammatory drugs.

The numbers and types of expressed chymases and chymase-like enzymes vary substantially among different species, such as primates, dogs, ruminant mammals, and rodents [12,13]. In humans, monkeys, dogs, and guinea pigs there is only a single functional chymase expressed, whereas sheep contain three chymases (designated as MCP1, MCP2 and MCP3) and hamsters contain two chymases (designated as HAM1 and HAM2). By contrast, in mice and rats the chymase loci underwent a major expansion to over 20 gene products [3,13,14]. Phylogenetically, the chymase family is divided into two subfamilies, α-chymases and β-chymases [12,13,15]. The genomes of primates, dogs, ruminants, and rodents are known to contain only one functional α-chymase, whereas rodents typically have multiple β-chymases. The precise biological rationale for this extensive duplication in the chymase gene is not yet understood. However, it has been proposed that gene duplication is important in the process of speciation, especially related to functions, such as immunity and sense of smell and taste, which may provide selective advantages in a novel environment [13].

☆ This article is dedicated to the memory of our long-time colleague Hongchang Ma, who died suddenly on April 12, 2010.

* Corresponding author. Tel.: +1 610 321 0799.
** Corresponding author. Tel.: +1 215 628 5812; fax: +1 215 628 4985.
E-mail addresses: jukkakervinen@comcast.net (J. Kervinen), Ldegarav@its.jnj.com (L. de Garavilla).
[1] These authors contributed equally to this work.

0006-2952/$ – see front matter © 2010 Elsevier Inc. All rights reserved.
doi:10.1016/j.bcp.2010.06.014

Most known chymases show chymotrypsin-like cleavage specificity, strongly preferring aromatic amino acids, Tyr and Phe, at the P1 substrate position (Schechter and Berger nomenclature [16]). Human α-chymase, as well as rodent β-chymases rat mast cell protease-1 (rMCP1) and mouse mast cell protease-4 (mMCP4), are examples of well-characterized enzymes with chymotrypsin-like substrate specificity [12,17,18]. Interestingly, chymases have demonstrated substrate-cleaving specificity beyond the canonical chymotryptic-type. For example, an opossum chymase was found to have a strong preference for Trp over Phe and Tyr at the P1 position [19]. In the case of the rodent α-chymases mMCP5, rMCP5 and HAM2, there is expanded diversification of substrate specificity by virtue of their preference for small aliphatic amino acids at P1, which makes them distinctly elastolytic in function [20–22]. Similarly, guinea pig chymase turned out to be Leu-specific at P1 [23]. Some insight into the shift in P1 specificity has been gleaned from X-ray structural and other studies. Notably, the amino acid at position 216, which is located on the wall of the S1 pocket and controls access to the pocket, has a profound effect on the specificity of chymotrypsin and related proteases [24–26]. A detailed map of the active-site residues involved in catalysis for human chymase was revealed by the structural work with enzyme–inhibitor complexes [27–30] and pro-chymase [31]. Structural analysis of HAM2 in complex with a peptidyl inhibitor showed that the elastolytic activity of rodent α-chymases derives from three unique residues, Asn189, Val190 and Val216, which form a narrow and shallow S1 pocket that can accommodate only small hydrophobic amino acids, such as Val or Ala [21]. Conversely, in human α-chymase and rodent β-chymases, the larger S1 pocket can accommodate Phe in the P1 position [30].

The wide variation in structure and function of a particular drug target across species can complicate the selection of the appropriate animal models to reliably evaluate drug candidates, in seeking to define the relative potency and efficacy for human clinical studies [2,3,32]. In the case of targeting human chymase, it would be beneficial to have a cross-species profile so as to appreciate what experimental animal models could be applied in the drug discovery process. Herein, we describe the production of eight recombinant mammalian chymases, along with the determination of their enzyme kinetic parameters. We have examined a series of active-site-directed human chymase inhibitors across these eight enzymes *in vitro* to characterize the variability of their inhibitory potency. Additionally, we determined the X-ray structure of human chymase complexed with the potent, selective inhibitor JNJ-18054478. This study provides novel information on interspecies potency variation that should facilitate the selection of animal models in chymase inhibitor research.

2. Materials and methods

2.1. Expression and purification of chymases

Chymase sequences were retrieved from the SwissProt/TrEMBL under the following accession numbers: human (P23946), macaque (P56435), dog (P21842), sheep MCP2 (P79204), sheep MCP3 (O46683), guinea pig (P85201), HAM1 (O08732) and HAM2 (O70164). The synthetic genes encoding mature active forms of chymases were purchased from DNA 2.0 (Menlo Park, CA). The genes were subcloned into a pAcGP67B vector that encodes a secretion signal, ubiquitin and an enterokinase (EK) cleavage sequence immediately before cloning site [33]. The human chymase gene in a pAcGP67B vector was kindly provided by Prof. Norman M. Schechter (University of Pennsylvania, Philadelphia, PA). The expression of human, macaque, dog, guinea pig, HAM1 and HAM2 chymases in baculovirus-infected insect cells (High Five™) (Invitrogen, Carlsbad, CA), purification on heparin–Sepharose (GE Healthcare, Piscataway, NJ), and activation by EK (Roche, Nutley, NJ) followed the protocol already described in detail [21]. After activation, the second heparin–Sepharose column was used to remove EK and released N-terminal peptides. An additional purification step on phenylbutylamine resin [33] was added for human chymase lots that were used for X-ray studies (we noticed that better diffracting crystals were obtained if this step was included in the purification protocol). Sheep MCP2 had a lower affinity to heparin than other chymases and numerous impurities were present after the first heparin–Sepharose purification step. Thus, before activation, a hydrophobic interaction step on Phenyl HP (GE Healthcare) was included. After Phenyl HP and activation by EK, the solution was loaded onto the second heparin–Sepharose column to obtain the final purity. Since sheep MCP3 had no affinity to heparin–Sepharose, anion exchange on Q HP (GE Healthcare) and Phenyl HP were used as the first two purification steps. After activation by EK, the second Q HP was used to obtain the final purity, where the active MCP-3, now with higher p*I* due to removal of the N-terminal sequence containing Asp-Asp-Asp-Asp-Lys, eluted in the flow-through.

2.2. Activity assays

Chromogenic *para*-nitroaniline (*p*NA) substrates were purchased from Bachem (King of Prussia, PA, USA). Substrate stock solutions were prepared in Me_2SO (DMSO) at 200–500 mM, and diluted either in 0.45 M Tris–HCl, pH 8.0, 1.8 M NaCl, 0.1% polyethylene glycol 8000 (TNP buffer) or 0.05 M Hepes, pH 7.5, 0.2 M NaCl, 0.05% octyl-β-D-glucopyranoside (OGP buffer). For determination of kinetic parameters, substrate concentrations ranged from 0.031 to 4 mM Suc-Ala-Ala-Pro-Phe-*p*NA for human, macaque, dog, sheep MCP2, sheep MCP3, and HAM1, 0.6–40 mM Suc-Ala-Ala-Pro-Ala-*p*NA for HAM2, and 0.16–20 mM Suc-Ala-Ala-Pro-Leu-*p*NA for guinea pig chymase. Reactions in 100 μL volume were performed in half-area 96-well Costar 3695 assay plates (Corning Inc., Corning, NY) at 37 °C, and DMSO was included at a final assay concentration of 5%. Reaction kinetics were monitored spectrophotometrically at 405 nm with a Spectramax plate reader (Molecular Devices, Sunnyvale, CA), and initial velocities were employed in the determination of kinetic parameters. An extinction coefficient of 9900 M^{-1} cm^{-1} was used for *p*NA cleaved from substrate at a path length of 0.55 cm.

2.3. Inhibition of chymases

Five test compounds, JNJ-31001958, JNJ-10311795, JNJ-18003414, JNJ-28838017, and JNJ-18054478 (Fig. 3), were synthesized in our laboratories [27,28]. Test compounds were assessed for inhibitory activity toward chymases from different species by kinetic analysis using *p*NA chromogenic substrates monitored at 405 nm, as described in Section 2.2. In half-area 96-well Costar 3695 assay plates, 90 μL of substrate in assay buffer was preincubated at 37 °C for 10 min with 5 μL test compound in DMSO to obtain final test compound concentrations that bracketed the K_i. Reactions were initiated by addition of 5 μL chymase. Initial velocities were determined by examination of the initial linear portion of the reactions. Plots of v_o/v_i vs. inhibitor concentration, where v_o = velocity without inhibitor, and v_i = inhibited velocity, were fit to a linear regression line, and IC_{50} was determined from the reciprocal of the slope. Alternatively, IC_{50}s were determined using GraphPad Prism® software (GraphPad Software, La Jolla, CA) and a four-parameter logistics equation. K_i was calculated from IC_{50} according to $K_i = IC_{50} \times (1/(1 + [S]/K_m))$, where [S] is the substrate concentration in the assay, and K_m is the Michaelis constant for the substrate [34]. For inhibition assays, substrate

concentrations employed were at or below the K_m for each enzyme–substrate pair. Within-run assay coefficient of variation (CV) was generally <10%; between-run CV <20%.

2.4. Crystallization, data collection, and structure determination

Purified human chymase (~10 mg/mL) in 10 mM Bis–Tris–HCl, pH 8.5, 50 mM NaCl, was complexed with JNJ-18054478 in a 1:2 molar ratio and screened for crystallization using the hanging-drop vapor diffusion method. Crystals formed at 25 °C from a solution containing 45% methanol, 0.1 M sodium malonate (pH 4). The crystals were transferred to a cryoprotectant solution containing 47% methanol, 0.1 M sodium malonate (pH 4), and, 30% glycerol. The crystals were then mounted and quickly frozen by immersion in liquid nitrogen. X-ray diffraction data to a resolution of 1.8 Å were collected at the IMCA-CAT ID-32 beamline at the Argonne National Laboratory. Diffraction data were indexed, integrated and scaled using the HKL suite [35]. The crystals belong to the $I2_3$ space group with one molecule in the asymmetric unit (Table 1). The structure was determined by molecular replacement with CNX [36] using the previously determined structure of human chymase (PDB accession code 1PJP) [30] as the search model. Model building was performed using O [37] and Coot [38]. Refinement and map calculations were carried out using PHENIX [39]. The atomic coordinates and structure factors (PDB 3N7O) have been deposited in the Protein Data Bank Research Collaboratory for Structural Bioinformatics, Rutgers University, New Brunswick, NJ (http://www.rcsb.org/), for immediate release.

2.5. Protein analysis

Protein concentration was measured with BioRad Protein Assay Reagent (BioRad Labs, Hercules, CA) relative to a standard curve prepared with bovine serum albumin. SDS-PAGE was carried out on precast NuPAGE 4–12% Tris–glycine gels (Invitrogen, Carlsbad, CA) and proteins were stained with Simply Blue Coomassie Stain (Invitrogen).

Table 1
Data collection and refinement statistics for human chymase in complex with JNJ-18054478.

Data collection	
Space group	$I2_3$
Wavelength (Å)	1.0
Resolution (Å)	1.8
Unique reflections	29,831
Redundancy	9.2
Completeness (%) (last shell)	99.9 (100)
I/σ (last shell)	37.1 (7.47)
*R*sym (%) (last shell)	4.7 (25.6)
Refinement	
Cell constants	$a=b=c=124.47$
Non-hydrogen atoms	1827
Water molecules	162
Resolution range (Å)	39.36–1.80
Reflections in refinement	28,721
R-factor[a] (%)	18.27
*R*free[b]	20.99
Root mean square deviations from ideal	
Bond lengths (Å)	0.008
Bond angles (°)	1.219
Ramachandran plot	
Preffered regions (%)	96.3
Allowed regions (%)	3.6
Disallowed region (%)	0.0

[a] *R*-factor__*h k l*_Fo_ _ k_Fc_/_*h k l*_Fo_.
[b] *R*free__*h k l* Test_Fo_ _ k_Fc_/_*h k l* Test_Fo_.

3. Results

3.1. Production of recombinant chymases

All chymases were expressed in baculovirus-infected insect cells and most of the enzymes were purified as described in detail for hamster chymases [21]. Sheep MCP2 required an additional chromatography step on Phenyl HP to obtain better purity. Sheep MCP3 did not have affinity to heparin and thus was purified with an alternate purification method. Following purification, all the fully mature chymases (25–28 kDa) were ≥95% pure as determined by SDS-PAGE (Fig. 1) and the correct N-termini were confirmed by N-terminal sequencing. Mass spectral analysis (data not shown) suggested that human, macaque, dog, sheep MCP2 and MCP3 and guinea pig chymases are heterogeneously glycosylated. As previously analyzed [21], HAM2 is also heterogeneously glycosylated, but no glycan side chains are attached to HAM1. Sheep MCP2, guinea pig chymase and HAM1 underwent minor autodegradation during purification, as smaller molecular weight polypeptides were detected by SDS-PAGE (Fig. 1).

3.2. Kinetic evaluation

The catalytic activities of the purified chymases were determined using chromogenic substrates (Table 2). Kinetic values for human chymase, HAM1 and HAM2 were determined previously [21]. The widely used human chymase substrate, Suc-Ala-Ala-Pro-Phe-*p*NA, was also suitable for macaque, HAM1, dog, and sheep chymases MCP2 and MCP3, whereas Suc-Ala-Ala-Pro-Ala-*p*NA was employed for HAM2, and Suc-Ala-Ala-Pro-Leu-*p*NA was employed for guinea pig chymase. The kinetic properties K_m, k_{cat}, and k_{cat}/K_m were determined in high (TNP buffer) and low (OGP buffer) salt conditions (Table 2). High-salt conditions are often used to measure human chymase activity [33,40], whereas the low-salt buffer represents physiologically more relevant conditions. The highest catalytic efficiency (k_{cat}/K_m) under these conditions and substrates was obtained with human and macaque enzymes, followed by dog and HAM1 chymase. These enzymes showed K_m values of 0.15–0.50 mM in high-salt and 0.36–0.87 mM in low-salt conditions, and turnover rates ranging from 15 to 93 s^{-1}. Although sheep MCP2 and MCP3 also cleaved Suc-Ala-Ala-Pro-Phe-*p*NA, the catalytic efficiency was 10–20% of human chymase. Cleavage of Suc-Ala-Ala-Pro-Phe-*p*NA was not significantly apparent with HAM2 or guinea pig chymase, but relatively low catalytic

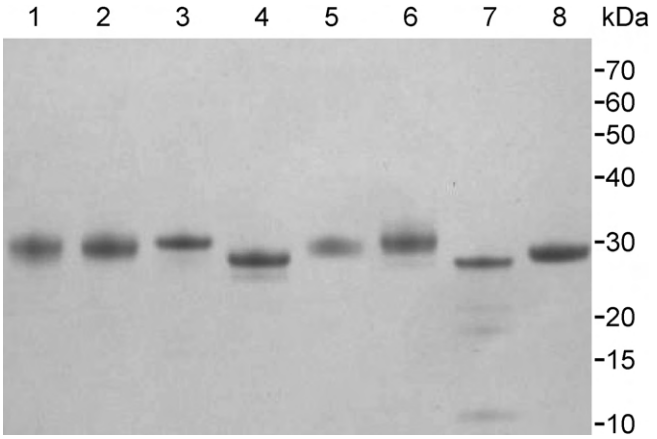

Fig. 1. SDS-PAGE for purified recombinant chymases. Human (lane 1), macaque (lane 2), dog (lane 3), sheep MCP2 (lane 4), sheep MCP3 (lane 5), guinea pig (lane 6), HAM1 (lane 7) and HAM2 (lane 8). Sample proteins (2 μg each) were analyzed in a 4–12% SDS-PAGE and detected with Coomassie blue.

Table 2
Kinetic parameters for recombinant chymases acting on Suc-Ala-Ala-Pro-Xaa-*p*NA, where Xaa denotes to the varied P1 substrate residue, in high (TNP) and low (OGP) salt conditions as described in Section 2.2.

Chymase source	Assay buffer	P1 substrate residue	Enzyme concentration (nM)	K_m (mM)	k_{cat} (s^{-1})	k_{cat}/K_m ($M^{-1}\,s^{-1}$)
Human[a]	TNP	Phe	0.7	0.38	93.1	245,000
	OGP	Phe	2	0.87	59.2	68,046
Macaque	TNP	Phe	1.5	0.15	39.2	261,333
	OGP	Phe	5.8	0.36	15.0	41,667
Dog	TNP	Phe	4	0.44	26.9	61,136
	OGP	Phe	10	0.43	8.6	20,000
Sheep MCP2	TNP	Phe	3	1.78	45.6	25,618
	OGP	Phe	9	1.58	23.4	14,810
Sheep MCP3	TNP	Phe	5	1.70	36.2	21,294
	OGP	Phe	10	1.22	13.2	10,820
Guinea pig	TNP	Leu	100	n.a.	n.a.	n.a.
	OGP	Leu	100	~20[b]	~1.3	~65[b]
Hamster HAM1[a]	TNP	Phe	3	0.50	25.9	51,800
	OGP	Phe	9	0.64	18.8	29,375
Hamster HAM2[a]	TNP	Ala	40	10.8	5.6	519
	OGP	Ala	40	23.5	5.2	221

n.a., not available due to substrate insolubility (see text).
[a] Data from J Biol Chem 283, 427–36, 2008.
[b] K_m value extrapolated due to substrate insolubility >20 mM (see text).

efficiencies were obtained with Suc-Ala-Ala-Pro-Ala-*p*NA and Suc-Ala-Ala-Pro-Leu-*p*NA, respectively.

It was recently shown that the guinea pig chymase is inactive toward Suc-Ala-Ala-Pro-Phe-*p*NA; however, it cleaves after Leu with a k_{cat}/K_m value of 600 $s^{-1}\,M^{-1}$ for Suc-Ala-Ala-Pro-Leu-*p*NA [23]. We confirmed the cleavage specificity for guinea pig chymase by testing Suc-Ala-Ala-Pro-Leu-*p*NA in high-salt and low-salt conditions, and activity was approximately 2-fold higher in high-salt buffer (Fig. 2). We also tested cleavage of insulin B-chain as earlier described for HAM1 and HAM2 [21]. Guinea pig chymase cleaved insulin B-chain after Leu15 and Leu17 and no other cleavage sites were detected up to 20 h of incubation (data not shown). In our attempts to determine catalytic efficiency using Suc-Ala-Ala-Pro-Leu-*p*NA, however, no saturation of the progress curve could be obtained at substrate concentrations up to 10 mM in TNP buffer and up to 20 mM in OGP buffer (Fig. 2) due to the solubility limit of the substrate. Thus, determination of accurate catalytic values was not possible in this case.

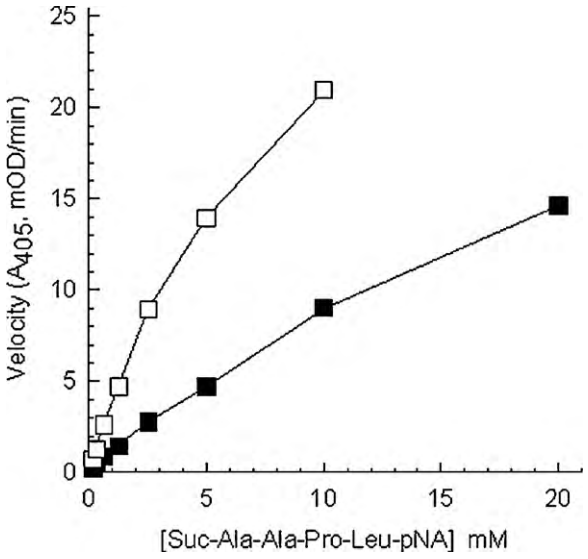

Fig. 2. Determination of initial velocity for guinea pig chymase as a function of substrate concentration in high (□) (TNP buffer) and low (■) (OGP buffer) conditions as described in Section 2.2.

3.3. Potency of chymase inhibitors across species

We examined a series of nonpeptide human chymase inhibitors, which include β-ketophosphonate JNJ-10311795, a potent dual inhibitor of human chymase and cathepsin G [27], and β-carboxamido-phosphon(in)ic acids [28] (Fig. 3). As an estimate of potential chymase inhibition in animal models, the potencies of these five human chymase inhibitors were determined *in vitro* against eight chymases from six species. The inhibitor potencies were tested under low-salt (Table 3) and high-salt (Table 4) conditions to determine any difference in inhibition due to a more physiological-like buffer, relative to the high-salt buffer. Under low-salt conditions (OGP buffer), most of the compounds showed enhanced or similar inhibition compared to high-salt conditions (TNP buffer), and the results discussed below refer to data obtained from low-salt conditions.

All the five test compounds showed potent human chymase inhibition with K_i values of ≤72 nM. JNJ-31001958, JNJ-10311795, and JNJ-18003414 inhibited human and macaque chymases with K_i values of 0.4–2 nM (apparent assay limit of quantification was 1 nM for human chymase and 3 nM for macaque). The K_i values for the other compounds were under 100 nM. However, significantly lower affinity was observed for all compounds when tested against chymases from the other species. Several-fold weaker compound inhibition was detected with dog, sheep MCP2, and HAM1 chymases, and little to no inhibition was observed with sheep MCP3, guinea pig, and HAM2 chymases.

3.4. X-ray structure and inhibitor binding

Human chymase was co-crystallized with JNJ-18054478 in an attempt to better understand the molecular basis for the potent inhibition of this compound and the potential cross-species differences. An X-ray structure of the complex was determined to a resolution of 1.8 Å. Throughout the present text the chymotrypsinogen [41] residue numbering scheme is used for the human chymase molecule and in the deposited PDB file. The

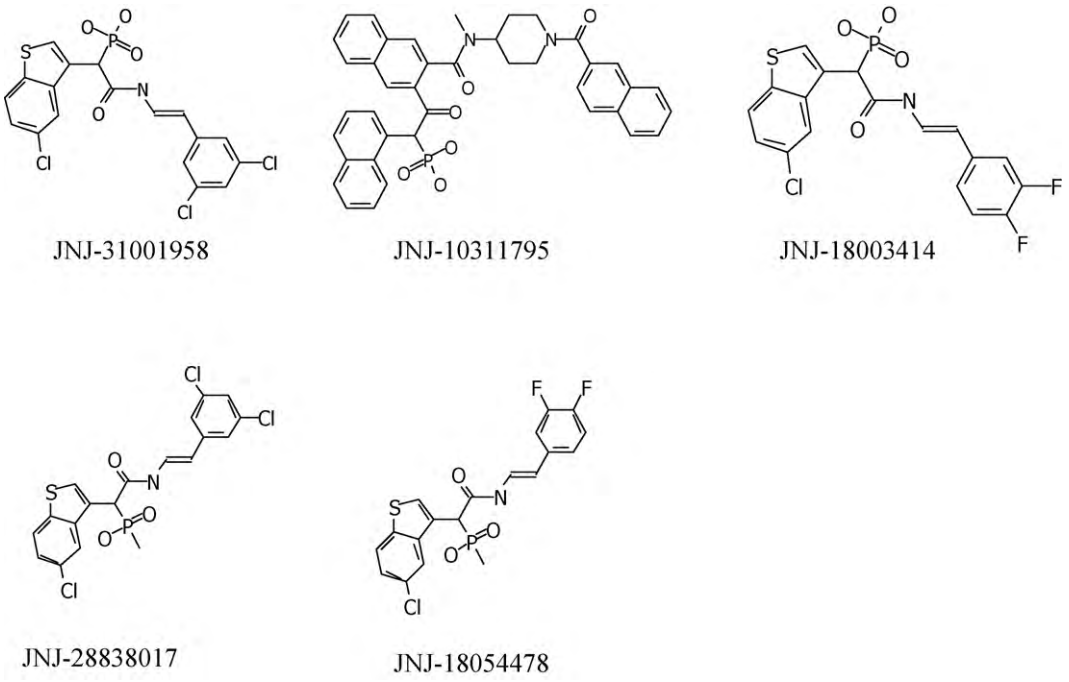

Fig. 3. Chemical structures of chymase inhibitors.

Table 3
Compound potency against chymases in low-salt conditions (OGP buffer) as described in Section 2.3.

Compound	Human K_i (nM)	Macaque K_i (nM)	Dog K_i (nM)	Sheep MCP2 K_i (nM)	Sheep MCP3 K_i (nM)	Guinea pig K_i[a] (nM)	HAM1 K_i (nM)	HAM2 K_i[b] (nM)
JNJ-31001958	0.4[c]	0.5[c]	68	73	>12,700	~4300	46	>16,600
JNJ-10311795	0.8[c]	2[c]	150	54	>12,700	~570	12	>16,600
JNJ-18003414	1.6	1.7[c]	340	490	>12,700	>11,400	370	>16,600
JNJ-28838017	13	10	480	720	>12,700	>11,400	410	>16,600
JNJ-18054478	72	57	1800	4900	>12,700	>11,400	3000	>16,600

[a] Substrate: Suc-Ala-Ala-Pro-Leu-*p*NA. K_i is an approximation due to extrapolation of substrate K_m.
[b] Substrate Suc-Ala-Ala-Pro-Ala-*p*NA.
[c] Approximate value due to plateau at low concentrations. Assay limit of quantification estimated as approximately 0.5 nM for human chymase and 1.5 nM for macaque in OGP buffer.

Table 4
Compound potency against chymases in high-salt conditions (TNP buffer) as described in Section 2.3.

Compound	Human K_i (nM)	Macaque K_i (nM)	Dog K_i (nM)	Sheep MCP2 K_i (nM)	Sheep MCP3 K_i (nM)	Guinea pig K_i[a] (nM)	HAM1 K_i (nM)	HAM2 K_i[b] (nM)
JNJ-31001958	2	1.7	300	1300	>14,200	>11,400	210	>13,600
JNJ-10311795	2.9	3.2	1700	530	>14,200	>11,400	190	>13,600
JNJ-18003414	15	15	1900	5700	>14,200	>11,400	2100	>13,600
JNJ-28838017	11	11	480	2300	>14,200	>11,400	440	>13,600
JNJ-18054478	69	74	2700	9800	>14,200	>11,400	5000	>13,600

[a] Substrate: Suc-Ala-Ala-Pro-Leu-*p*NA.
[b] Substrate Suc-Ala-Ala-Pro-Ala-*p*NA.

human chymase structure consists of one molecule in the asymmetric unit containing residues 16–245 with a break in the electron density between residues 126 and 128 (the break in the electron density was likely due to cleavage at Phe127, which is the major site of autolysis in human chymase). The structure includes two glycosylated asparagines (Asn72 and Asn95) with two N-acetyl-glucosamine groups attached to each Asn. There is also a malonic acid molecule from the crystallization buffer on the surface of the protein between residues Arg161, Asn185, and Lys186.

In human α-chymase, the inhibitor binding region is defined by residues Lys40, His57, Tyr94, Asn95, Thr96, Leu99, Asp102, Ala190, Phe191, Lys192, Gly193, Ser195, Val213, Ser214, Tyr215, Gly216 and Arg217 (Fig. 4). The region is mostly polar because of main chain carbonyls that are arranged along the surface of the region. Although the inhibitor is present as a racemic mixture, only the *S* enantiomer is bound in the chymase catalytic site. The inhibitor ligand has its benzothiophene group in the S1 substrate binding pocket and its difluoro-phenyl group in S2. The placement of the methyl vs. the oxygen for the phosphinic acid group was determined based on B values and the H-bond network between the inhibitor and the protein. Several residues are involved in hydrogen bond interactions with the methyl-phosphinic acid group (His57, Gly193, Ser195, and Lys40) and with the amino

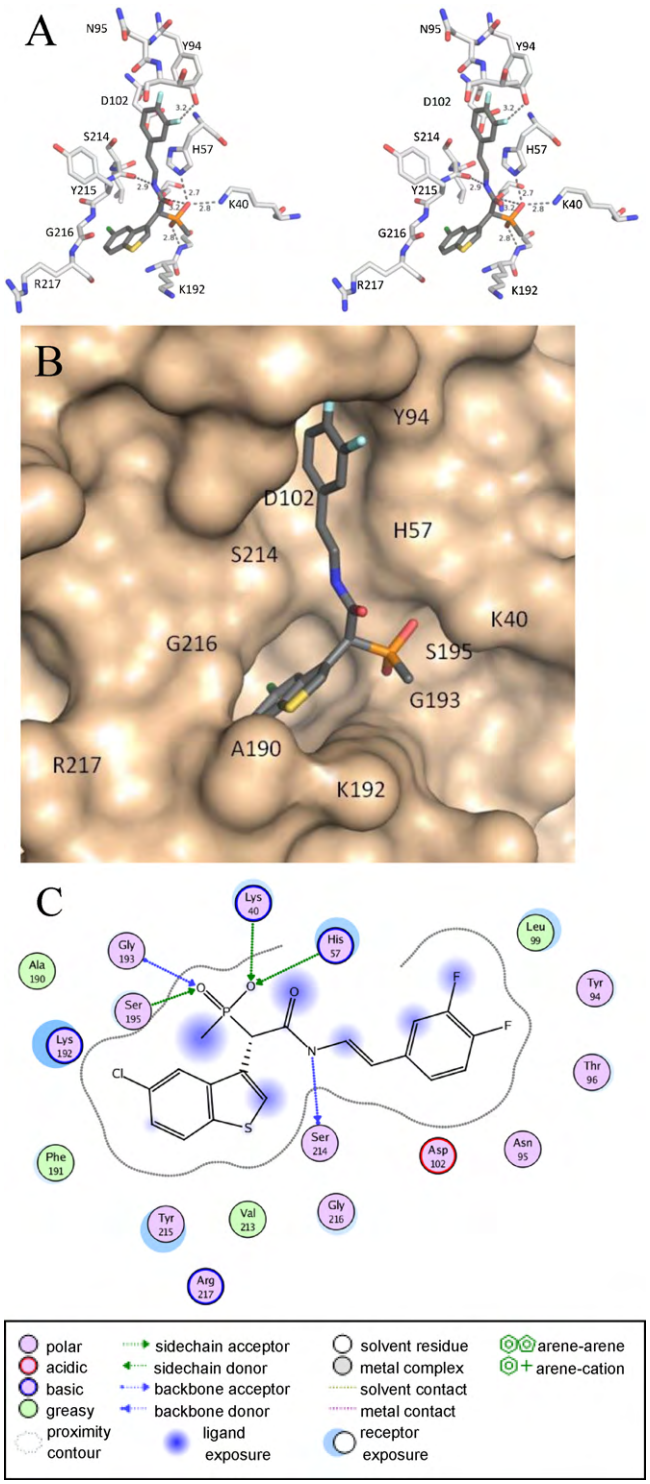

Fig. 4. X-ray co-crystal structure of human chymase complexed with JNJ-18054478. (A) Stereo diagram of the interactions between human chymase and the compound. The compound is shown with atoms colored by element; carbon grey, nitrogen blue, oxygen red, sulfur yellow, phosphorous orange, chlorine green, and fluorine light blue. (B) Surface representation of the catalytic site of human chymase in complex with the inhibitor. Figure was made using PyMOL (DeLano Scientific LLC, The PyMOL Molecular Graphics System, Palo Alto, CA, www.pymol.org). (C) Schematic representation of the interactions between human chymase and JNJ-18054478. This graphic was made by using MOE (Chemical Computing Group, http://www.chemcomp.com). (For interpretation of the references to color in this figure legend, the reader is referred to the web version of the article)

group (Ser214). The carbonyl of Ser214 hydrogen bonds (2.93 Å) to the amino group of the inhibitor. Tyr94 forms a weak electrostatic interaction (3.2 Å) with the meta-fluorine in S2.

4. Discussion

Animal models play an important role in the preclinical development of potential drugs. Recently, highly potent inhibitors against human chymase have been discovered and characterized [28,42–44]. In advancing such agents to human clinical studies, it is necessary to ascertain their pharmacological actions in suitable animal models of disease. To better direct preclinical animal testing for our chymase inhibitors, we determined the potencies of test compounds against eight chymases from six species *in vitro*. The major finding of our work was the markedly wide variation of inhibitor potency across species. As expected, all the compounds were highly potent inhibitors (K_i values from ~0.4 to 72 nM) of human and macaque chymases, highly similar enzymes with only six residue changes in the mature proteins and only one (Ser218 in human; Leu218 in macaque) in the substrate binding region from residues 186 to 229 [21,45]. However, compound potencies were significantly lower for dog, sheep MCP2, and HAM1 chymases, despite phylogenetic proximity to the human enzyme [12,13]. The key similarities include (a) identical active-site residues Ser189, Ala190, Gly216, and Ala226, which are known to be critical for the substrate selectivity and hydrolysis [24–26], and (b) all the enzymes readily hydrolyzed a common chymase substrate, Suc-Ala-Ala-Pro-Phe-*p*NA. Despite these analogies, the compound potencies for dog, sheep MCP2, and hamster HAM1 chymases were 10–300-fold weaker compared to potencies for human and macaque enzymes. Sheep MCP3, which is structurally and functionally related to cattle duodenase [46], was not inhibited by the test compounds. Likewise, guinea pig chymase, which is specific for Leu at P1 [23] and HAM2 chymase, an elastolytic chymase [21], were not inhibited by the compounds. In some cases, it has been shown that the kinetic efficiency against chromogenic substrates can be greatly affected by only one or a few amino acid changes, and in some utmost instances these changes have been enough to convert chymase specificity into elastolytic activity, and *vice versa* [22,23,47]. Thus, subtle variations in residues within the active-site cavity can drastically affect substrate specificity and, as we have now shown, the inhibitory potency of small-molecule inhibitors.

Here we show that the compound JNJ-18054478 forms a hydrogen-bonding network with residues Lys40, His57, Gly193, Ser195, and Ser214 and the aryl analog occupies the hydrophobic S2 pocket (Fig. 4). Specifically the side chain of Lys40 makes a strong hydrogen bond (2.74 Å) with the hydroxyl group of the compound. Previously we published the binding mode of JNJ-10311795 with human chymase [27]. This ligand forms a hydrogen-bonding network with residues Lys40, His57, Lys192, Gly193, and Ser195 in the S1 substrate pocket and the 1-naphthyl group tightly occupies the hydrophobic S2 pocket. Interestingly, when the human chymase sequence is aligned with the dog, sheep MCP2, and HAM1 counterparts, the human chymase residues that form a hydrogen-bonding network with JNJ-18054478 and JNJ-10311795, are almost identical in all these mammalian chymases. The only exception is Lys40 that, in the dog chymase and HAM1, is Ala40 [48] and sheep MCP2 occupy Val at the position 40. Is variation in this residue enough to influence inhibitor binding as profoundly as shown here? Some evidence exists that the residue at the position 40 has an important role in the enzyme catalysis. Human chymase has been identified as an efficient angiotensin (AT) converting enzyme, selectively hydrolyzing AT I at Phe8 to generate bioactive AT II [48,49]. Site-specific mutagenesis study [48] has shown that Lys40 in human chymase influences substrate

recognition resulting in cleavage at Phe8 in AT. When Lys40 was mutated for Ala, the human enzyme became much less sensitive for hydrolysis at Phe8 of AT whereas Tyr4 hydrolytic rates (destructs bioactivity of AT II) were enhanced 16-fold compared to the wild-type human enzyme. Thus, based on these studies, Lys40 has an important role in the substrate recognition and hydrolysis. However, to what extent residue 40 affects the compound potency remains to be elucidated.

The crystal structure of HAM2 complexed to the inhibitor MeOSuc-Ala-Ala-Pro-Ala-chloromethylketone revealed a narrow and shallow S1 substrate pocket (largely influenced by Val216 compared to Gly216 in human chymase) that cannot accommodate a benzyl side chain of Phe at P1 position [21]. Similarly, benzothiophene group of JNJ-18054478 that accommodates S1 substrate pocket in human chymase (Fig. 4) is obviously too large to fit the S1 pocket of HAM2 and apparently explains the lack of potency of this and other compounds in the same series against HAM2 and also against guinea pig chymase. Sheep MCP3 was not inhibited by any of the compounds either even though it contains Gly at 216 and it hydrolyzes Suc-Ala-Ala-Pro-Phe-*p*NA, although ~10-fold lower rate compared to human chymase (Table 2). Lack of potency and lower hydrolytic rate may be explained by other subtle active-site residue changes than the residue at position 216. Residues at 189 and 190 also directly influence the size of the S1 substrate binding pocket [21]. In human, macaque and dog chymases, sheep MCP2 and HAM1 the residues are Ser189 and Ala190 whereas sheep MCP3 contains a negatively charged Asp189 and a bulkier Ser190 compared to Ala. These residue differences may cause the lower rate of Suc-Ala-Ala-Pro-Phe-*p*NA hydrolysis and lack of compound potency in sheep MCP3 although further experiments are needed to test this hypothesis in detail.

Chymase has been increasingly linked to a number of cardiovascular and inflammatory diseases, and numerous animal models in various species (including mice, rats, hamsters, sheep, and dogs) have been utilized for pharmacological characterization of inhibitors [32,43,44,50–52]. A large family of chymase-like gene products expressed in mice and rats has hampered compound evaluation, especially since some of the rodent enzymes depart significantly from human chymase in function [14]. However, some studies have been carried out in mice, such as involvement of mouse MCP4 (mMCP4), the closest counterpart to the human chymase [18], in autoimmune arthritis. In both collagen-induced and passive-model arthritis, the clinical scores were significantly reduced in the mMCP4$^{-/-}$ animals compared to mMCP4$^{+/+}$ controls, indicating a pathogenic role of mMCP4 in autoimmune disease [53]. Another study showed that chymase is involved in the development of angiotensin II-induced abdominal aortic aneurysm in apoE-deficient mice and that the disease progression was prevented by administering a chymase inhibitor NK3201 [54]. Also, chymase inhibitor SUN13834 was found to improve dermatitis in NC/Nga mice, which spontaneously develop dermatitis resembling atopic dermatitis [44]. On the contrary, a recent study with wild-type mice and mice lacking mMCP4 showed that mMCP4 may also have a protective role in allergic airway inflammation [55]. Nevertheless, since mice and rats contain numerous chymases with various functions, it has been difficult to extrapolate results obtained in these rodent species to humans. Thus, a highly desirable objective has been to identify another animal species with only one or a limited number of chymases with well-characterized hydrolytic properties akin to human chymase.

Hamsters have been used as an experimental species in numerous studies to assess the efficacy of human chymase inhibitors for treating various diseases. For example, TEI-E548 was tested in a hamster myocardial infarction model. The authors report that TEI-E548 inhibited recombinant human and hamster chymase, purified from hamster tongue, with K_i values of 6 and 31 nM, respectively, and showed efficacy in treating symptoms related to myocardial infarction [56]. Another study in hamsters showed that chymase inhibitor TY-51469 provides pancreatic islet protection in hamsters with steptozotocin-induced diabetes [43]. Chymase inhibitor NK3201 was effective in the prevention of pulmonary fibrosis in hamsters [57] and chymase inhibitors may also provide a therapeutic target in the stabilization of atherosclerotic plaques [58]. In our laboratories, the dual chymase/cathepsin G inhibitor, JNJ-10311795 (also known as RWJ-355871), was tested in a hamster pulmonary inflammation model, and the results show promising therapeutic utility for treating airway inflammatory diseases that involve mechanisms dependent on cathepsin G and/or chymase [27,50]. In support of these *in vivo* results, JNJ-10311795 potently inhibited HAM1 *in vitro* with a K_i value of 12 nM (Table 3). In another study, JNJ-10311795 was administered orally in a carrageenan-induced hamster model of inflammation and showed marked anti-inflammatory activity [28]. Taken together, several studies suggest that hamsters could be a potential animal model in the assessment of effectiveness of human chymase inhibitors. However, several human chymase inhibitors showed markedly lower potency against HAM1 compared to the human counterpart, while HAM2 remained unaffected (Tables 3 and 4). Thus, for any novel human chymase inhibitor, it is important to test the potency against purified HAM1 *in vitro* to better comprehend its effectiveness in this animal model.

Guinea pigs apparently contain only one chymase, belonging to the α-chymase class. However, a recent study [23] and our results show that guinea pig chymase cleaves primarily after Leu, making it an unusual chymase compared to its counterparts. In addition, human chymase inhibitors from our compound series showed little inhibition against guinea pig chymase. Thus, guinea pigs seem to be of questionable utility for the characterization of human chymase inhibitors.

In some chymase inhibitor studies, like in vascular proliferation and prevention of vascular diseases, larger animals like dogs [59] and sheep [50] have been studied. Out of the three known chymases in sheep, MCP2 is the closest counterpart to the human enzyme and some of the human chymase inhibitors tested here also showed reasonable potency against sheep MCP2 (Tables 3 and 4). However, because of the existence of three chymases with unique kinetic properties and differences in the substrate specificity, it would be challenging to use sheep for accurate compound characterization. Based on our *in vitro* findings, macaques (and presumably other non-human primates) ought to be a favorable species to study human diseases that are associated with chymase activity.

5. Conclusion

We have expressed, purified, and characterized chymases from humans, macaques, dogs, sheep (MCP2 and MCP3), guinea pigs, and hamsters (HAM1 and HAM2). Five nonpeptide compounds known to be potent inhibitors of human chymase were tested against a total of eight recombinant chymases from five species. The results of this profiling unquestionably illustrate that human chymase inhibitors show a wide variation in potency against the enzymes from different species. Our results point to the importance of careful *in vitro* analysis of compounds to select appropriate animal models in support of advancing chymase inhibitors to human clinical studies and to better interpret results from studies in animal models in terms of the potential for treating human inflammatory, autoimmune, and cardiovascular diseases.

Acknowledgements

We thank Keli Dzordzorme for excellent technical assistance in cloning of the chymases. Use of the beamline ID-32 with beamline management and support provided by the IMCA-CAT staff at the Advanced Photon Source was supported by the companies of the Industrial Macromolecular Crystallography Association through a contract with the Center for Advanced Radiation Sources at the University of Chicago. Use of the Advanced Photon Source was supported by the U.S. Department of Energy, Office of Science, Office of Basic Energy Sciences, under Contract No. W-31-109-Eng-38.

References

[1] Theoharides TC, Kempuraj D, Tagen M, Conti P, Kalogeromitros D. Differential release of mast cell mediators and the pathogenesis of inflammation. Immunol Rev 2007;217:65–78.
[2] Caughey GH. Mast cell tryptases and chymases in inflammation and host defense. Immunol Rev 2007;217:141–54.
[3] Trivedi NN, Caughey GH. Mast cell peptidases: chameleons of innate immunity and host defense. Am J Respir Cell Mol Biol 2010;42:257–67.
[4] Bradding P, Walls AF, Holgate ST. The role of the mast cell in the pathophysiology of asthma. J Allergy Clin Immunol 2006;117:1277–84.
[5] Andoh A, Deguchi Y, Inatomi O, Yagi Y, Bamba S, Tsujikawa T, et al. Immunohistochemical study of chymase-positive mast cells in inflammatory bowel disease. Oncol Rep 2006;16:103–7.
[6] Ong PY. Emerging drugs for atopic dermatitis. Expert Opin Emerg Drugs 2009;14:165–79.
[7] Kovanen PT. Mast cells: multipotent local effector cells in atherothrombosis. Immunol Rev 2007;217:105–22.
[8] Sun J, Zhang J, Lindholt JS, Sukhova GK, Liu J, He A, et al. Critical role of mast cell chymase in mouse abdominal aortic aneurysm formation. Circulation 2009;120:973–82.
[9] Schechter NM, Plotnick M, Selwood T, Walter M, Rubin H. Diverse effects of pH on the inhibition of human chymase by serpins. J Biol Chem 1997;272:24499–507.
[10] Belkowski SM, Boot JD, Mascelli MA, Diamant Z, de Garavilla L, Hertzog B, et al. Cleaved secretory leucocyte protease inhibitor as a biomarker of chymase activity in allergic airway disease. Clin Exp Allergy 2009;39:1179–86.
[11] Belkowski SM, Masucci J, Mahan A, Kervinen J, Olson M, de Garavilla L, et al. Cleaved SLPI, a novel biomarker of chymase activity. Biol Chem 2008;389:1219–24.
[12] Caughey GH. New developments in the genetics and activation of mast cell proteases. Mol Immunol 2002;38:1353–7.
[13] Gallwitz M, Hellman L. Rapid lineage-specific diversification of the mast cell chymase locus during mammalian evolution. Immunogenetics 2006;58:641–54.
[14] Puente XS, Lopez-Otin C. A genomic analysis of rat proteases and protease inhibitors. Genome Res 2004;14:609–22.
[15] Chandrasekharan UM, Sanker S, Glynias MJ, Karnik SS, Husain A. Angiotensin II-forming activity in a reconstructed ancestral chymase. Science 1996;271:502–5.
[16] Schechter I, Berger A. On the size of the active site in proteases. I. Papain. Biochem Biophys Res Commun 1967;27:157–62.
[17] Andersson MK, Enoksson M, Gallwitz M, Hellman L. The extended substrate specificity of the human mast cell chymase reveals a serine protease with well-defined substrate recognition profile. Int Immunol 2009;21:95–104.
[18] Andersson MK, Karlson U, Hellman L. The extended cleavage specificity of the rodent beta-chymases rMCP-1 and mMCP-4 reveal major functional similarities to the human mast cell chymase. Mol Immunol 2008;45:766–75.
[19] Reimer JM, Enoksson M, Samollow PB, Hellman L. Extended substrate specificity of opossum chymase—implications for the origin of mast cell chymases. Mol Immunol 2008;45:2116–25.
[20] Karlson U, Pejler G, Tomasini-Johansson B, Hellman L. Extended substrate specificity of rat mast cell protease 5, a rodent alpha-chymase with elastase-like primary specificity. J Biol Chem 2003;278:39625–31.
[21] Kervinen J, Abad M, Crysler C, Kolpak M, Mahan AD, Masucci JA, et al. Structural basis for elastolytic substrate specificity in rodent alpha-chymases. J Biol Chem 2008;283:427–36.
[22] Kunori Y, Koizumi M, Masegi T, Kasai H, Kawabata H, Yamazaki Y, et al. Rodent alpha-chymases are elastase-like proteases. Eur J Biochem 2002;269:5921–30.
[23] Caughey GH, Beauchamp J, Schlatter D, Raymond WW, Trivedi NN, Banner D, et al. Guinea pig chymase is leucine-specific: a novel example of functional plasticity in the chymase/granzyme family of serine peptidases. J Biol Chem 2008;283:13943–51.
[24] Gallwitz M, Reimer JM, Hellman L. Expansion of the mast cell chymase locus over the past 200 million years of mammalian evolution. Immunogenetics 2006;58:655–69.
[25] Perona JJ, Craik CS. Evolutionary divergence of substrate specificity within the chymotrypsin-like serine protease fold. J Biol Chem 1997;272:29987–90.
[26] Wouters MA, Liu K, Riek P, Husain A. A despecialization step underlying evolution of a family of serine proteases. Mol Cell 2003;12:343–54.
[27] de Garavilla L, Greco MN, Sukumar N, Chen ZW, Pineda AO, Mathews FS, et al. A novel, potent dual inhibitor of the leukocyte proteases cathepsin G and chymase: molecular mechanisms and anti-inflammatory activity in vivo. J Biol Chem 2005;280:18001–7.
[28] Greco MN, Hawkins MJ, Powell ET, Almond Jr HR, de Garavilla L, Hall J, et al. Discovery of potent, selective, orally active, nonpeptide inhibitors of human mast cell chymase. J Med Chem 2007;50:1727–30.
[29] McGrath ME, Mirzadegan T, Schmidt BF. Crystal structure of phenylmethanesulfonyl fluoride-treated human chymase at 1.9 Å. Biochemistry 1997;36:14318–24.
[30] Pereira PJ, Wang ZM, Rubin H, Huber R, Bode W, Schechter NM, et al. The 2.2 Å crystal structure of human chymase in complex with succinyl-Ala-Ala-Pro-Phe-chloromethylketone: structural explanation for its dipeptidyl carboxypeptidase specificity. J Mol Biol 1999;286:163–73.
[31] Reiling KK, Krucinski J, Miercke LJ, Raymond WW, Caughey GH, Stroud RM. Structure of human pro-chymase: a model for the activating transition of granule-associated proteases. Biochemistry 2003;42:2616–24.
[32] Miyazaki M, Takai S, Jin D, Muramatsu M. Pathological roles of angiotensin II produced by mast cell chymase and the effects of chymase inhibition in animal models. Pharmacol Ther 2006;112:668–76.
[33] Wang Z, Walter M, Selwood T, Rubin H, Schechter NM. Recombinant expression of human mast cell proteases chymase and tryptase. Biol Chem 1998;379:167–74.
[34] Cheng Y, Prusoff WH. Relationship between the inhibition constant (K1) and the concentration of inhibitor which causes 50 per cent inhibition (I50) of an enzymatic reaction. Biochem Pharmacol 1973;22:3099–108.
[35] Otwinowski Z, Minor W. Processing of X-ray diffraction data collected in oscillation mode. Methods Enzymol 1997;276:307–26.
[36] Brunger AT, Adams PD, Clore GM, DeLano WL, Gros P, Grosse-Kunstleve RW, et al. Crystallography & NMR system: a new software suite for macromolecular structure determination. Acta Crystallogr D Biol Crystallogr 1998;54:905–21.
[37] Jones TA, Zou JY, Cowan SW, Kjeldgaard M. Improved methods for building protein models in electron density maps and the location of errors in these models. Acta Crystallogr A 1991;47:110–9.
[38] Emsley P, Cowtan K. Coot: model-building tools for molecular graphics. Acta Crystallogr D Biol Crystallogr 2004;60:2126–32.
[39] Adams PD, Grosse-Kunstleve RW, Hung LW, Ioerger TR, McCoy AJ, Moriarty NW, et al. PHENIX: building new software for automated crystallographic structure determination. Acta Crystallogr D Biol Crystallogr 2002;58:1948–54.
[40] Caughey GH, Raymond WW, Wolters PJ. Angiotensin II generation by mast cell alpha- and beta-chymases. Biochim Biophys Acta 2000;1480:245–57.
[41] Wang D, Bode W, Huber R. Bovine chymotrypsinogen, a X-ray crystal structure analysis and refinement of a new crystal form at 1.8 A resolution. J Mol Biol 1985;185:595–624.
[42] Doggrell SA, Wanstall JC. Vascular chymase: pathophysiological role and therapeutic potential of inhibition. Cardiovasc Res 2004;61:653–62.
[43] Takai S, Jin D, Ohzu M, Tanaka K, Miyazaki M. Chymase inhibition provides pancreatic islet protection in hamsters with streptozotocin-induced diabetes. J Pharmacol Sci 2009;110:459–65.
[44] Terakawa M, Fujieda Y, Tomimori Y, Muto T, Tanaka T, Maruoka H, et al. Oral chymase inhibitor SUN13834 ameliorates skin inflammation as well as pruritus in mouse model for atopic dermatitis. Eur J Pharmacol 2008;601:186–91.
[45] Krem MM, Rose T, Di Cera E. Sequence determinants of function and evolution in serine proteases. Trends Cardiovasc Med 2000;10:171–6.
[46] McAleese SM, Pemberton AD, McGrath ME, Huntley JF, Miller HR. Sheep mast-cell proteinases-1 and -3: cDNA cloning, primary structure and molecular modelling of the enzymes and further studies on substrate specificity. Biochem J 1998;333:801–9.
[47] Solivan S, Selwood T, Wang ZM, Schechter NM. Evidence for diversity of substrate specificity among members of the chymase family of serine proteases. FEBS Lett 2002;512:133–8.
[48] Muilenburg DJ, Raymond WW, Wolters PJ, Caughey GH. Lys40 but not Arg143 influences selectivity of angiotensin conversion by human alpha-chymase. Biochim Biophys Acta 2002;1596:346–56.
[49] Lorenz JN. Chymase: the other ACE? Am J Physiol Renal Physiol 2010;298:F35–6.
[50] Maryanoff BE, de Garavilla L, Greco MN, Haertlein BJ, Wells GI, Andrade-Gordon P, et al. Dual inhibition of cathepsin g and chymase is effective in animal models of pulmonary inflammation. Am J Respir Crit Care Med 2010;181:247–53.
[51] Matsumoto C, Hayashi T, Kitada K, Yamashita C, Miyamura M, Mori T, et al. Chymase plays an important role in left ventricular remodeling induced by intermittent hypoxia in mice. Hypertension 2009;54:164–71.
[52] Palaniyandi SS, Nagai Y, Watanabe K, Ma M, Veeraveedu PT, Prakash P, et al. Chymase inhibition reduces the progression to heart failure after autoimmune myocarditis in rats. Exp Biol Med (Maywood) 2007;232:1213–21.
[53] Magnusson SE, Pejler G, Kleinau S, Abrink M. Mast cell chymase contributes to the antibody response and the severity of autoimmune arthritis. FASEB J 2009;23:875–82.
[54] Inoue N, Muramatsu M, Jin D, Takai S, Hayashi T, Katayama H, et al. Effects of chymase inhibitor on angiotensin II-induced abdominal aortic aneurysm

development in apolipoprotein E-deficient mice. Atherosclerosis 2009; 204:359–64.
[55] Waern I, Jonasson S, Hjoberg J, Bucht A, Abrink M, Pejler G, et al. Mouse mast cell protease 4 is the major chymase in murine airways and has a protective role in allergic airway inflammation. J Immunol 2009;183: 6369–76.
[56] Hoshino F, Urata H, Inoue Y, Saito Y, Yahiro E, Ideishi M, et al. Chymase inhibitor improves survival in hamsters with myocardial infarction. J Cardiovasc Pharmacol 2003;41(Suppl. 1):S11–8.
[57] Sakaguchi M, Takai S, Jin D, Okamoto Y, Muramatsu M, Kim S, et al. A specific chymase inhibitor, NK3201, suppresses bleomycin-induced pulmonary fibrosis in hamsters. Eur J Pharmacol 2004;493:173–6.
[58] Guo T, Chen WQ, Zhang C, Zhao YX, Zhang Y. Chymase activity is closely related with plaque vulnerability in a hamster model of atherosclerosis. Atherosclerosis 2009;207:59–67.
[59] Furubayashi K, Takai S, Jin D, Muramatsu M, Ibaraki T, Nishimoto M, et al. The significance of chymase in the progression of abdominal aortic aneurysms in dogs. Hypertens Res 2007;30:349–57.